Exp Fluids (2009) 46:765–775
DOI 10.1007/s00348-008-0595-0

RESEARCH ARTICLE

Wing–wake interaction reduces power consumption in insect tandem wings

Fritz-Olaf Lehmann

Received: 26 June 2008 / Revised: 11 November 2008 / Accepted: 12 November 2008 / Published online: 9 December 2008

Abstract Insects are capable of a remarkable diversity of flight techniques. Dragonflies, in particular, are notable for their powerful aerial manoeuvres and endurance during prey catching or territory flights. While most insects such as flies, bees and wasps either reduced their hinds wings or mechanically coupled fore and hind wings, dragonflies have maintained two independent-controlled pairs of wings throughout their evolution. An extraordinary feature of dragonfly wing kinematics is wing phasing, the shift in flapping phase between the fore and hind wing periods. Wing phasing has previously been associated with an increase in thrust production, readiness for manoeuvrability and hunting performance. Recent studies have shown that wing phasing in tandem wings produces a twofold modulation in hind wing lift, but slightly reduces the maximum combined lift of fore and hind wings, compared to two wings flapping in isolation. Despite this disadvantage, however, wing phasing is effective in improving aerodynamic efficiency during flight by the removal of kinetic energy from the wake. Computational analyses demonstrate that this increase in flight efficiency may save up to 22% aerodynamic power expenditure compared to insects flapping only two wings. In terms of engineering, energetic benefits in four-wing flapping are of substantial interest in the field of biomimetic aircraft design, because the performance of man-made air vehicles is often limited by high-power expenditure rather than by lift production. This manuscript provides a summary on power expenditures and aerodynamic efficiency in flapping tandem wings by investigating wing phasing in a dynamically scaled robotic model of a hovering dragonfly.

F.-O. Lehmann (✉)
BioFuture Research Group, University of Ulm,
Albert-Einstein-Allee 11, 89081 Ulm, Germany
e-mail: fritz.lehmann@uni-ulm.de

1 Introduction

Flying insects are known for their impressive flight agility, manoeuvrability and endurance, including low speed hovering, effective gliding flight and sudden variation in flight speed and altitude. In the past, multiple experimental and computational studies have shown, how insects enhance their lift production to support body weight, to lift loads, and to allow manoeuvring flight (e.g. Birch and Dickinson 2003; Dickinson et al. 1999; Lan and Sun 2001; Lehmann et al. 2005; Ramamurti and Sandberg 2007; Srygley and Thomas 2002; Sun and Tang 2002; Wang et al. 2003). The discovery of the various unsteady aerodynamic mechanisms for lift enhancement such as leading edge vortex development, rotational circulation and wake capture has considerably improved our knowledge and has highlighted the complexity of flapping flight compared to fixed-wing aircraft performance.

Despite the difficulties in improving lift coefficients for flight, many insects are limited by power rather than by the ability of the flapping wings to support body weight. Aerodynamic efficiency in flapping flight is of considerable interest, because some insects such as the small fruit fly *Drosophila* may fly for several hours without food intake. Other species, such as the parasitic wasp *Nasonia*, even completely abstain from feeding as adults (King 1993; Langellotto et al. 2000). This is remarkable, because in this species the females perform elaborate and long-lasting search flights for oviposition. Comparatively few studies have addressed the potential trade-off between high-lift

production and high-energetic costs during flight, and adjustments in wing kinematics have mostly been discussed in terms of maximum lift production rather than in terms of the benefits in energetic costs. Considering flapping flight from the perspective of power expenditure and aerodynamic efficiency is thus of great ecological significance in order to understand the evolution of kinematic patterns used by birds, bats and insects.

Experimental work on tethered insects suggests that most of the chemical energy stored in the food is wasted as heat in the flight musculature and as horizontal, non-weight supporting drag during wing flapping (Casey and Ellington 1989; Ellington 1984a, 1985). The efficiency with which the insect flight muscle converts chemical energy from sugar and fat into muscle mechanical power is low and typically scattered around 10% (for a review see Lehmann 2001). This value holds for the two major types of flight muscles used by flying insects: the asynchronous, indirect flight muscle (IFM) mostly found in flies, bees, and beetles, and the synchronous, direct flight muscle (SFM) of dragonflies, butterflies and many other insects. The IFM contracts in response to passive lengthening (stretch activation) during high-frequent thorax oscillations and is deactivated by fibre shortening (shortening deactivation, Moore 2006). It inserts large-scale at the thorax walls. By contrast, the SFM is closely controlled by its neural drive and attached to the wing base. This muscle moves the wing by pulling directly on the wing's lever arm. In contrast to insects, muscle efficiency of the vertebrate flight muscle in birds and bats is slightly higher and ranges from 10 to 40% (Lehmann 2001). Aerodynamic efficiency, in turn, defines how much mechanical power is required to move the wings in each flapping cycle compared to the power required to produce aerodynamic lift. In engineering terms, flight muscle mechanical power output in an insect corresponds to the shaft power of a rotating propeller. The latter efficiency is typically expressed by the ratio between the minimum power requirements for flight (Rankine–Froude power) and the aerodynamic power expenditure, and typically amounts to values scattered around 25–35% total chemical energy (Ellington 1984a). Together, this yields a relatively low total flight efficiency of not more than 3–5% in the insect species investigated so far (Lehmann 2001).

Widely neglected aspects in assessing the efficiency of flapping flight are kinematic manoeuvres in which flow conditions change due to the interference between wings. Wing–wake interaction during the dorsal stroke reversal is probably the most prominent manoeuvre in two-winged flight (Lehmann et al. 2005; Weis-Fogh 1973). In four-winged insects, such as dragonflies, the fore wing experiences change in flow conditions due to the inwash of fluid caused by the nearby hind wing, and the hind wing must cope with the downwash produced by the flapping fore wing. These dependencies, moreover, vary during manoeuvring flight, since a wide range of phase relationships has been described between fore and hind wings. High flight forces have been correlated to in-phase flapping of fore and hind wing, but in many cases dragonflies also operate with wing motion somewhat out of phase (Alexander 1984; Norberg 1975; Reavis and Luttges 1988; Rüppell 1989; Thomas et al. 2004; Wakeling and Ellington 1997a; Wang et al. 2003). A total antiphase motion in which fore and hind wings are phase-shifted by 50% of the stroke cycle might promote hunting performance, either by increasing the readiness for manoeuvrability, or by reducing the centre of body mass oscillations, thereby aiding location of targets and reducing the insect's visibility to potential prey (Grodnitsky 1999).

Computational and experimental studies on the consequences of wing phasing have demonstrated that phase has a bearing on both thrust production and power consumption (Lan 1979; Luttges 1989; Wang and Russell 2007). Moreover, flow visualizations around dragonfly model wings have shown some of the potential consequences of wing–wake interaction including the fusion of vortices, leading edge vortex destruction and wake capture effects (Maybury and Lehmann 2004, Saharon and Luttges 1987, 1988, 1989). However, the implications of these fluid dynamic effects in terms of power expenditure and aerodynamic efficiency have remained widely unclear. Lan's (1979) computational study on heaving and pitching plates predicted that interacting tandem wings may produce high thrust with high efficiency due to energy extraction by the hind wing from the wake of the fore wing. Although the latter study is not strictly applicable to hovering flight and neglects the impediments of flow separation in slow dragonfly flight (Thomas et al. 2004), it is tempting to conclude that wing kinematic patterns in four-winged insects should be shaped by both lift production and energy expenditure (Usherwood and Lehmann 2008). Moreover, measurements show that wing phasing in four wings produces higher transient forces and thus larger transient moments than in two wings (Maybury and Lehmann 2004). Depending on their temporal distribution within the stroke cycle, these extremes potentially help to improve manoeuvrability and stability of an insect.

In this paper, we analyse how dragonflies may reduce energetic costs during flight by adjusting the timing of wing motion between their two pairs of wings and discuss why efficiency of the insect flight apparatus might be a more pertinent measure for flapping flight than lift production. This is achieved by calculations of induced and aerodynamic power requirements for flapping flight at various phase shifts, estimations of the significance of wing hinge separation for the ratio of combined drag to lift production, and quantification of the wake below dragonfly model wings. The experimental force data used for these

analyses are those collected by Maybury and Lehmann (2004) who focused on force development rather than on energetic aspects during wing phasing. In sum, the present study tries to strengthen the emerging unified approach between biology and aeronautical engineering in the field of unsteady aerodynamics and energetics of flying animals.

2 The mechanical dragonfly model

The dynamically scaled, electromechanical dragonfly model mimicked wing-wake interactions during hovering flight of a generic dragonfly at intermediate Reynolds numbers (*Re*, Fig. 1). We employed an averaged kinematic pattern derived from various species, in order to demonstrate the significance of hovering for power requirements and efficiency with a range of fore-hind wing phases. Orientation of stroke planes and wing motion broadly followed the observations on free-flight hovering of *Sympetrum sanguineum*, a common species in dragonfly research (Wakeling and Ellington 1997a). The robotic fore and hind wings were stacked vertically, separated by 1.25 chord length (48 mm) between the wing hinges, and flapped with symmetrical downstroke and upstroke in a horizontal stroke plane (Fig. 1a). Flapping amplitude was 100°, flapping frequency 0.533 Hz, and feathering angle at mid-half stroke was 45° (Fig. 1b). Supination and pronation at the stroke reversals occurred during the initial and final 10% of each half-stroke, flipping the wings by 90°. Fore-hind wing phases are described as the percentage of the stroke cycle, at which the hind wing leads the fore wing: 0% indicates in-phase stroking, +25% (−25%) indicates that the hind (fore) wing leads by a quarter stroke cycle, and 50% indicates total anti-phase.

To avoid too many morphological parameters confounding the results, we used flat, non-corrugated wings made from 2 mm thick Plexiglas for both force and particle image velocimetry (PIV) measurements. Wing mass of fore and hind wing was 11.0 and 13.4 g, and mean spanwise flexural stiffness *EI* yielded 0.11 and 0.29 Nm^2 for the two wings, respectively. For comparison, spanwise flexural stiffness of insect wings ranges from approximately 10^{-6} Nm^2 in flies, to 10^{-4} Nm^2 in dragonflies and 0.5×10^{-3} Nm^2 in moths (Combes and Daniel 2003; Ganguli et al. 2008). To roughly compare these values in terms of wing deflection, we applied mean force production of the mechanical model (0.32 and 0.31 N, fore and hind wing, respectively) and one-quarter body weight of the dragonfly *Aeshna multicolor* (total weight = 754 mg) to the wing tips, respectively. According to Gordon (1978),

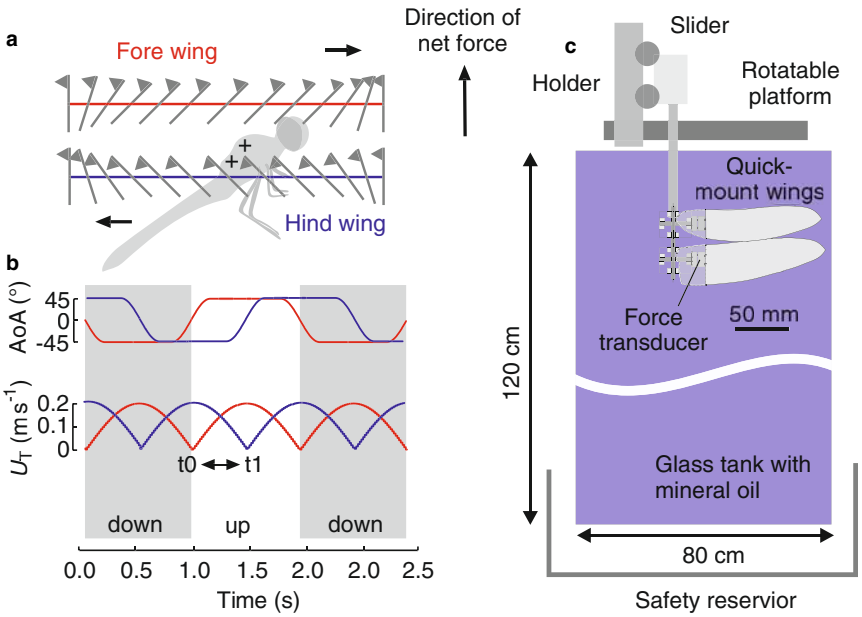

Fig. 1 Mechanical dragonfly model and wing shifting kinematics. **a** Body posture as reported for a hovering dragonfly by Wakeling and Ellington (1997a) and idealized wing tip path as used in the mechanical model of the fore- (*red*) and hind wing (*blue*). *Grey lines* show a travelling wing blade during the up (*lower wing*) and down stroke (*upper wing*). *Triangles* near the leading wing edge indicate the upper wing surface. **b** Alteration of geometric angle of attack (AoA) and translational wing velocity (U_T) based on flapping motion for both wings. The temporal difference between t_0 and t_1 indicates the kinematic phase shift between the fore- and hind wing stroke cycle. **c** Experimental setup showing gear boxes and wings of the mechanical model. The wings are stationary and immersed in a tank filled with mineral oil. Sizes of gears and wings are not to scale. *Scale bar* applies to the mechanical wings only

this resulted in a spanwise tip deflection of 1.02° (0.40°) for the model fore (hind) wing and 6.3° for the dragonfly wing. Wing planforms were based on the wings of the small dragonfly *Polycanthagyna melanictera* with low aspect ratios of 6.8 and 7.4 at spanwise lengths of 190 and 185 mm for the fore and hind wing, respectively (Fig. 1c).

Reynolds number based on the product between mean wing chord and wing tip velocity during wing flapping for the fore and hind wing was 105 and 125, respectively. Although these values are at the low end of small dragonflies (250–500, Rüppell 1989), they are considered well above the transitional Reynolds number of approximately 55 for vortex shedding (Miller and Peskin 2004; Vandenberghe et al. 2004). According to the Reynolds number of the hind wing, the flapping frequency of the mechanical model corresponds to a wing stroke frequency of approximately 40 Hz in air common for small dragonflies. Due to the sinusoidal velocity profile, the contribution of wing mass inertia to aerodynamic force at the stroke reversals is moderate and accounts for a maximum of 6% of the mean force produced by an isolated hind wing (0.21 N). According to previous calculations, the same holds for added mass inertia that produces transient force peaks at the stroke reversals of approximately 0.06 N or 30% of the measured mean force. Averaged throughout the entire stroke cycle, however, added mass inertia due to the wing's translational and rotational accelerations apparently amounts to less than 1% of the mean aerodynamic force production. We calculated added mass inertia using an analytical model for an infinitesimally thin 2D plate moving in an inviscid fluid modified towards 3D conditions (Sedov 1965; Sane and Dickinson 2001a, b; Maybury and Lehmann 2004).

Instantaneous forces such as weight-supporting lift in the vertical and drag parallel to horizontal motion were measured by 6 degrees-of-freedom force transducers (Nano 17, ATI, USA) attached to the wing bases of both wings. For each kinematic phase, we recorded a sequence of six cycles but averaged forces only from four stroke cycles (2–5) in order to avoid confounding effects from the initial downwash acceleration (Birch and Dickinson 2001). To allow 2D digital PIV, the model wings including motors, gears and force transducers were immersed in a 0.77 m^3 flow tank filled with highly viscous pharmaceutical white oil (density, 0.88×10^3 kg m^{-3}; kinematic viscosity, 120 cSt; Fig. 1c). Closest distance between wing tip and the lateral tank walls was approximately 20 cm; the fore wing stroke plane was approximately 95 cm above the bottom of the tank. Air bubbles as seeding particles reflected the light of the PIV laser (TSI, Insight 6.0) in a vertical slice situated half-way along the fore wing, highlighting flow conditions at mid down stroke. Each PIV experiment consisted of seven successive stroke cycles, but similar to the force measurements, only the flow fields from the last five cycles were recorded, averaged and analysed. In general, the aim of the mechanical model and the robotic kinematics was not to precisely copy a specific dragonfly, but to provide a reasonable test bed with which the significance of wing phasing for power requirements and aerodynamic efficiency could be investigated without too many confounding kinematics and aerodynamic factors such as changes in body position or alterations in the net flight force vector, respectively.

3 Lift and drag production in tandem wings

In the dragonfly model, the combined lift production of fore and hind wing varies with wing phasing, which widely concurs with previous computational studies on dragonfly flight (Sun and Lan 2004; Wang and Russell 2007; Fig. 2). At −25% phase shift, when the fore wing leads, fore wing lift only slightly decreases by at most 8% compared to a single wing, while hind wing lift is attenuated by more than 50% of the single wing performance (0.21 N, for combined lift see Fig. 2a). Most of this reduction in lift is due to a reduction of the aerodynamic angle of attack between each wing and the local fluid. Similar to tandem helicopters, the angle of attack is reduced by the downwash of the fore wing on the hind wing, and by the hind wing's inwash on the fore wing.

Particle image velocimetry yielded a second mechanism for lift reduction: the partial destruction of the leading edge vortex on the hind wing due to the proximity of fore wing's start vortex shed at the beginning of each half stroke. It has been shown that this vortex interaction attenuates vorticity in the leading edge vortex (LEV) of the hind wing by 31%, compared to a wing flapping in isolation (from 129 to 88.4 s^{-1}, Maybury and Lehmann 2004). Tandem wings restore *mean* lift close to the combined performance of wings flapping in isolation when the hind wing leads wing motion by +25% of the stroke cycle, although *instantaneous* lift and drag of the tandem hind wing differs from the performance of a single wing (Figs. 2a, 3). Particle image velocimetry shows that under these conditions, the leading edge vortex on the hind wing fully develops and the hind wing gains additional lift by recycling kinematic energy produced by the fore wing via a wake capture mechanism (Maybury and Lehmann 2004). In addition to the reduced lift with fore-hind wing interaction, the mean lift to mean drag ratio during wing phasing is not improved compared with wings flapping in isolation, although the ratio slightly increases with increasing drag production from 0.72 at 0.3 N to 0.85 at 0.6 N drag ($y = -0.077 + 0.98x$, $R^2 = 0.86$, $P < 0.0001$, $N = 40$, Fig. 4a). At first glance, it is thus tempting to conclude that wing phasing in dragonflies has primarily evolved to alter lift and drag for flight control rather than developed from an evolutionary pressure on power expenditure and thus flight efficiency.

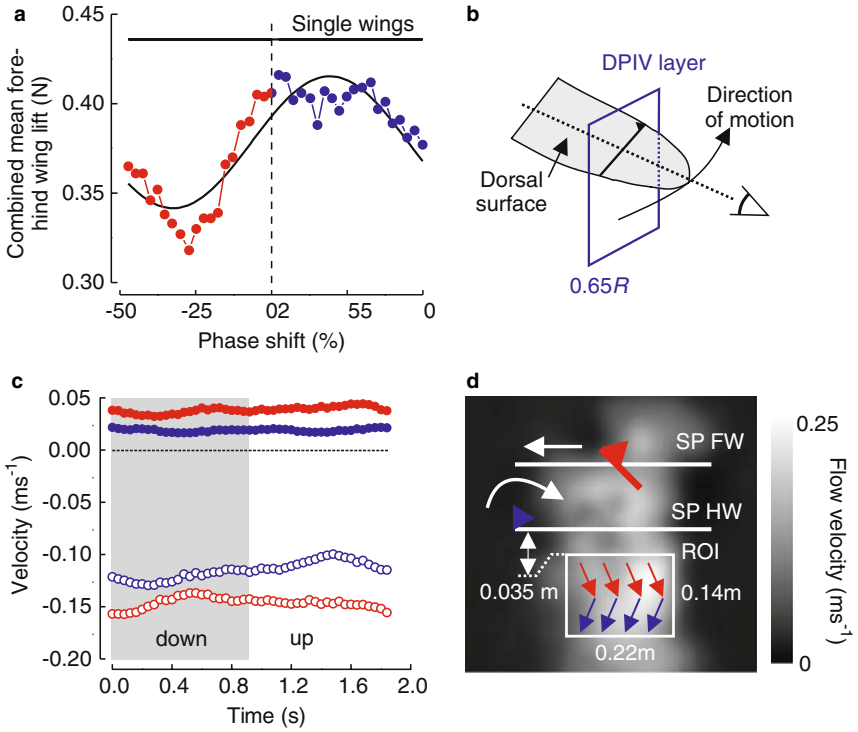

Fig. 2 Lift production and flow velocities in the wake below the hind wing averaged from 5 PIV image pairs, all recorded at mid down stroke (single point measurement at +25% stroke cycle). **a** Modulation in combined lift production during phase-shifting kinematics when either the fore wing (*red*) or the hind wing (*blue*) leads wing motion. **b** The two-dimensional layer for particle image velocimetry was orientated perpendicular to the longitudinal axis of the wing at mid half stroke. *R* wing length. **c** Vertical (*open circles*) and absolute horizontal velocity (*closed circles*) in the wake at mid half stroke, measured in a 224 mm × 140 mm (width × height) region-of-interest (ROI) below the hind wing. *Blue* (*red*) indicates +25% (−25%) phase shift when hind (fore) wing leads wing motion. **d** Fluid velocity (*grey scale*) at +25% phase shift, stroke planes of fore and hind wing, and location of the region-of-interest used for the measurements in **c**. See Fig. 7 for more detailed flow data. *SP* stroke plane, *FW* fore wing, *HW* hind wing

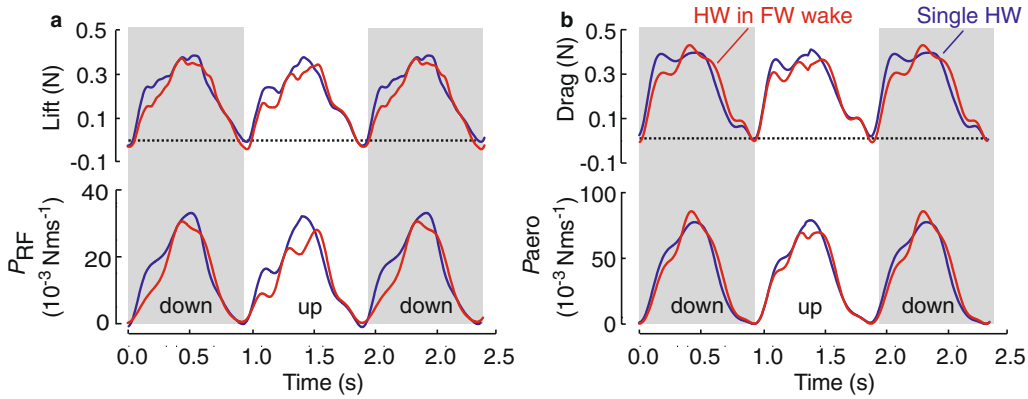

Fig. 3 Time traces of aerodynamic forces and power requirements. **a** Lift and Rankine–Froude power of a hind wing in tandem configuration (*red*) compared to forces and power of a hind wing flapping in isolation (*blue*). **b** Drag and aerodynamic power of the hind wing flapping in the downwash of the fore wing (*red*) and in a single hind wing (*blue*). P_{RF}, Rankine–Froude power; P_{aero}, aerodynamic power calculated from the product between drag and wing velocity. Wing separation between the wing hinges was 1.25 times mean chord width and wing phasing was +25% (hind wing leads by quarter stroke cycle). For abbreviations, see legend of Fig. 2

Previous work on tandem wings has shown that the modulation of combined lift and drag depends on several factors including wing size and the distance between the fore and hind wing stroke plane (Lehmann 2008). With increasing distance between both wings, phase shift for maximum lift production decreases due to vortex travel

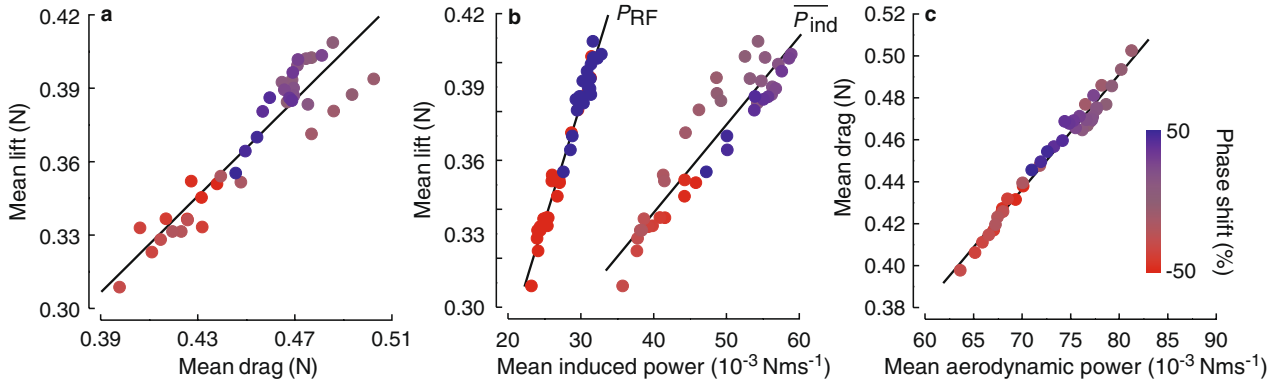

Fig. 4 Combined mean lift, drag and power requirements of both wings in dragonfly tandem wings plotted as a function of wing phasing. **a** Relationship between mean lift and mean drag. **b** Mean lift plotted against Rankine–Froude power (P_{RF}) according to Eq. 1 and mean induced power ($\overline{P_{ind}}$) calculated from the product between mean lift and mean induced velocity measured in the far wake below the hind wing. **c** Relationship between mean drag and mean aerodynamic power. Phase shift is indicated in pseudo colour (*blue* hind wing leads wing motion; *red* forewing leads wing motion). See text for more information on regression fit curves

time while the modulation of lift and drag increasingly disappears (Fig. 5). This effect is due to viscosity that smoothes out temporal and spatial fluctuation of the wake, eventually producing a downwash homogeneous in time and space. The mechanical dragonfly produces both maximum combined fore-hind wing lift at +25% phase and maximum lift modulation only when the wings are closest (Fig. 5b). Due to the increasing loss of vorticity and temporal variation in the wake with increasing wing separation, lift and drag approach the performance of wings flapping in isolation at a separation of approximately five chord lengths (Fig. 5b, c). The same holds for mean lift to mean drag ratio (Fig. 5d), together suggesting that besides other properties, the morphological distance between fore and hind wing hinge determines the animal's ability to produce and modulate lift using wing phasing kinematics.

4 Induced power during wing phasing

In his time-averaged approach towards insect flight energetics, Ellington (1984a) provided a numerical framework that allows calculations of power requirements for wing flapping based on averaged kinematics and mean lift production. Following Weis-Fogh's original work (Weis-Fogh 1972), Ellington divided the requirements for flight into

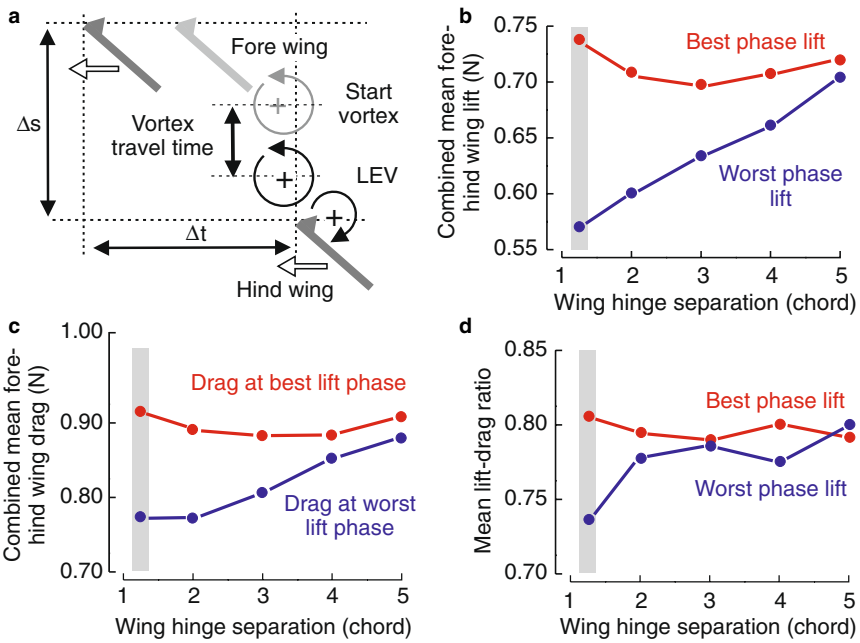

Fig. 5 Mean lift, mean drag and mean lift-to-drag ratio at best (+25%, *red*) and worst (−25%, *blue*) phase shift. **a** Schematic drawing illustrating −25% phase shift (Δt) and wing hinge separation (Δs). The phase shift for maximum lift decreases with increasing distance between both stroke planes for maximum lift production due to vortex travel time. **b** Combined fore-hind wing lift at best and worst phase shift plotted as a function of wing separation. **c** Combined drag at best and worst lift production and **d** mean lift to mean drag ratio. *Grey bar* closest distance between wing hinges; *LEV* leading edge vortex

three terms: inertial power needed to accelerate the wings in each half stroke, profile power necessary to cope with profile drag, and induced power required to produce a vertical momentum for weight support. Assuming that inertial costs are minimum due to elastic energy storage in the flight musculature, Ellington's conventional two-dimensional elementary blade approach defines total power requirements for flight as the sum of profile and induced power. The latter term represents the power associated with induced drag arising from the tilt of the relative velocity vector by the generated downwash.

Exact estimations of induced power are challenging, because this measure requires quantifications of induced velocity in the down wash of flapping wings. Figure 2c shows the temporal development of horizontal and vertical flow velocities within a flapping cycle of the mechanical model wings, measured in a region of interest, 35 mm below the hind wing stroke plane (plane covered by wing tip, Fig. 2d). These measures capture the flow regime at mid half stroke and approximately at the centre of force production of the wings (65% wing length). They should be considered as rough estimates because a three-dimensional flow field would be needed to fully quantify mean induced velocity with PIV. At minimum lift production at −25% phase shift (fore wing leads), mean vertical flow speed amounts to 0.146 ± 0.043 m s^{-1} (mean ± SD) compared to 0.115 ± 0.063 m s^{-1} (mean ± SD) at +25% phase shift (Fig. 2c). This suggests that despite higher lift production, there is less kinetic energy in the wake at best phase shift compared to worst phase conditions. Alternatively to PIV estimates, induced velocity may be derived from the velocity with which the start vortices shed by the fore wings travel downstream in the wake. A previous analysis scored this velocity using conventional video devices and derived a mean travel velocity of 0.082 m s^{-1}, which is approximately 56% of the free stream velocity of the vertical wake (Lehmann 2008).

The theoretical minimum of induced power in tandem wings of a quasi-steady jet is equal to the Rankine–Froude estimate of induced power normalized by a vortex shedding factor k_F that takes into account the periodicity of the wake due to wing flapping (Ellington 1984a). This factor is the ratio in the far wake of the Rankine–Froude velocity to the mean velocity of the periodic wake. The ideal Rankine-Froude power P_{RF} for an actuator disk produced by a hovering insect and ignoring unsteady aerodynamic mechanisms such as wake capture, is given by:

$$P_{RF} = L \cdot \left(\frac{1}{2} L \cdot \rho^{-1} A_0^{-1}\right)^{0.5}, \quad (1)$$

with L, the mean lift force acting directly upwards, ρ, the fluid density, and A_0, the actuator disc area, the area swept by the two wings. With vertically stacked wings operating with horizontal stroke planes, just as for coaxial rotors of helicopters, the flapping fore and hind wings form a single actuator disc. Under these assumptions, the same fluid is accelerated by both sets of wings. Following Ellington, and again considering only the two wings on the right body side of the dragonfly, the area of the appropriate actuator disc A_0 may be expressed by:

$$A_0 = \frac{1}{2}\Phi R^2, \quad (2)$$

where Φ is the stroke amplitude and R the wing length of the longer fore wing (0.19 m). Assuming that lift is proportional to the power raised to the exponent 2/3 (cf. Eq. 1), statistical analysis suggests that lift production increases with increasing Rankine-Froude power by a slope of 4.39 ($y = -0.04 + 4.39x^{2/3}$, $R^2 = 0.97$, $\chi^2 = 97.5 \times 10^{-5}$, DOF = 38, Fig. 4b). For comparison, mean lift increases with mean induced power $\overline{P_{ind}}$ (lift × induced velocity) with a slope of 1.96 ($y = 0.11 + 1.96x^{2/3}$, $R^2 = 0.87$, $\chi^2 = 38.8 \times 10^{-4}$, DOF = 38, Fig. 4b) based on the induced velocity measurements in Fig. 2c, and with a slope of 5.62 ($y = -0.18 + 5.62x^{2/3}$, $R^2 = 0.99$, $\chi^2 = 33.3 \times 10^{-7}$, DOF = 38) based on vortex travel time. Since Rankine-Froude power is the theoretical minimum, the vortex shedding factor must be greater than unity for a periodic wake: from the above data we derived 1.69 (Fig. 4b), and 1.08 assuming a uniform vortex travel velocity of 0.082 m s^{-1}. Consequently, the mean axial wake velocity in the far wake of the mechanical dragonfly model is approximately 41% ($k_F = 1.69$) and 7% ($k_F = 1.08$) less than the Rankine-Froude estimate of axial wake velocity.

5 Aerodynamic power during wing phasing

Instantaneous aerodynamic power is given by the product between instantaneous drag and wing velocity. Time traces of aerodynamic power P_{aero} for the hind wing in tandem configuration and a hind wing flapping in isolation are shown in Fig. 3b, whereas Fig. 4c shows the relationship between mean drag and mean aerodynamic power at the various phase shifts (allometric fit: $y = -0.15 + 3.45x^{2/3}$, $R^2 = 0.98$, $\chi^2 = 57.2 \times 10^{-5}$, DOF = 38, Fig. 4c). At +25% phase shift (hind wing leads) the difference in hind wing drag between single and tandem wing configuration appears to be minor, suggesting only small changes in power due to wing-wake interference at optimal conditions (mean drag, 0.239 vs. 0.239 N; mean aerodynamic power, 37.5×10^{-3} vs. 38.2×10^{-3} Nms^{-1}; isolated hind wing vs. hind wing in tandem configuration).

To calculate aerodynamic power savings during fore-hind wing interference, we estimated the wing beat

frequency required to achieve identical mean lifts (0.404 N) for wings operating at different phases. The scaling model is independent of the aerodynamic mechanism used for lift production and simply assumes that drag scales in proportion to lift, a reasonable assumption for the expected small change in Reynolds number. From these estimates, the power requirements for hovering were scaled by adjusting stroke frequency, while constraining wing shape and all remaining kinematic parameters. The analysis shows that hovering with a phase shift of +25% requires 16% less power than with a phase shift of −25% (fore wing leads). Although this comparison ignores other potential kinematic parameters, such as adjustments in stroke amplitude or angle of attack, it shows that hovering with the appropriate phase between both wings may have a considerable energetic significance. Moreover, compared to dragonfly wings flapping in isolation, hovering with four wings at +25% phase shift requires 22% less aerodynamic power than hovering only with the two fore wings at the same mean lift production. The increase in stroke frequency required to match the lift produced by a single fore wing to the combined lift of tandem wings (at 25% phase shift) amounts to approximately 0.18 Hz or 33% of the employed flapping frequency, while Reynolds number increases from 105 to 140.

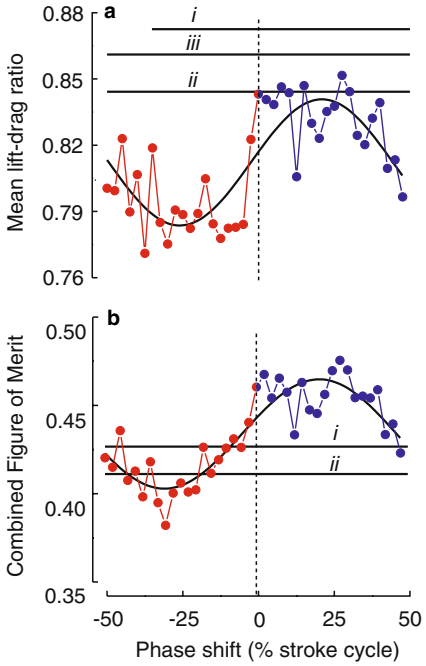

Fig. 6 **a** Ratio between mean lift and mean drag and **b** aerodynamic efficiency of total lift production expressed as Figure of Merit (FoM) during phase shifting kinematics of the mechanical dragonfly. Black solid lines show performance of isolated (*i*) fore wing, (*ii*) hind wing, and (*iii*) the cumulative effect of isolated fore and hind wings, and sine fit to the data as a function of kinematic phase

6 Aerodynamic efficiency (Figure of Merit)

Our instantaneous measurements of lift and drag circumvent Ellington's numerical framework on mean induced and mean profile power requirements in flapping wings, calculating aerodynamic power expenditure directly from the product between instantaneous drag and translational wing velocity. Aerodynamic efficiency is then represented by the Figure of Merit, FoM, a special case of propeller efficiency used for hovering helicopters. This term describes the ratio of the minimum theoretical power required to produce a vertical downward jet for hovering (Rankine–Froude power, Figs. 3a, 4b) to the measured aerodynamic power (Figs. 3b, 4c, Prouty 2005). Consequently, the Figure of Merit expresses the efficiency of flapping flight propulsion in comparison with an ideal hovering helicopter.

Similar to the mean lift and the ratio of mean lift to mean drag, aerodynamic efficiency varies with phase shift but is always below 50% of the efficiency of an ideal actuator disc or ideal helicopter (Fig. 6). Numerical predictions without flow separation (Lan 1979) and real helicopters (Prouty 2005) yield approximately twice the mean efficiency of the dragonfly tandem model. The low efficiency in the dragonfly model is due to its high aerodynamic power requirements and, therefore, consistent with the poor lift-to-drag ratio of low aspect ratio insect wings flapping at high geometrical angle of attack of approximately 30°–40° (Ellington 1984b). For comparison, wings of the fruit fly *Drosophila* produce a lift-to-drag ratio slightly above unity at best lift coefficient of 1.8 ($Re = 136$, Dickinson et al. 1999), and a continuously rotating replicate of a low aspect ratio hawkmoth wing reaches a lift-to-drag ratio of approximately 1.2 at its best lift coefficient of 1.15 ($Re = 8071$, Usherwood and Ellington 2002).

The poor lift-to-drag ratio in insects is part of a trade-off between high lift production for hovering and slow forward flight, and low energetic costs. Superficially, an insect could energetically benefit from a reduction in angle of attack during wing flapping at the cost of an increase in wing size or kinematic parameters such as stroke amplitude and stroke frequency. The latter modifications, however, potentially interfere with the limits of the flight apparatus: the mechanical limit of the thorax to move the wings at large flapping angles, the physiological limit on high-frequency muscle contraction, and the ability of flight muscle and associated proteins (e.g. resilin, Gorb 1999) to elastically store kinetic energy within each half stroke cycle. Simple numerical models on flight energetics suggest that elastic energy storage is beneficial during the wing's acceleration phases and thus in cases in which mean inertial power exceeds aerodynamic power requirements

(Dickinson and Lighton 1995). An increase in both wing mass (size) and stroke frequency would require an elevated capacity of the thorax for elastic energy recycling. Due to the difficulties in assessing metabolic rate during flight, however, it is difficult to prove such concepts in the behaving animal (e.g. Casey 1989, Feuerbacher et al. 2003; Josephson 1997; Lehmann and Dickinson 1997; Lehmann and Heymann 2006). Altogether, the numerous findings suggest that the evolution of wing kinematics and wing design in an insect depends on various aerodynamic and biological requirements and most likely reflects the best compromise between these needs.

The major reason for the poor performance—or efficiency—of an insect wing is the loss of leading edge suction force due to the development of a leading edge vortex at high angle of attack. In the dragonfly model, however, FoM clearly outscores the efficiency of wings flapping in isolation (FoM fore wing = 0.427, FoM hind wing = 0.411, Fig. 6b), significantly improving the overall energy budget during hovering in four-winged insects (Usherwood and Lehmann 2008). The apparent paradox that aerodynamic efficiency can be improved in tandem wings despite a slight reduction of lift-to-drag ratio compared to single wings can be explained by two different views describing the same physical phenomenon: a temporal shift in force production within the stroke cycle and a wake capture mechanism that removes lateral motion of the fluid by the hind wing. The periodic, non-vertical components of the wake produced by the fore wing allow, at positive phase shifts, the hind wing to produce lift when moving relatively slowly near the two stroke reversals. This view is supported by a previous study on dragonfly wings, showing that at +25% phase shift the hind wing experiences a gain in lift at 35 and 85% of the stroke cycle and thus toward the end of each half stroke, although the wing experiences maximum translational velocity at mid up and down stroke (sinusoidal velocity profile, Maybury and Lehmann 2004; Fig. 1). Thus, while the significance of lift and drag development is minor for mean lift and weight support, it may be considerable in terms of power and aerodynamic efficiency.

The second description of the mechanism causing an elevated FoM is apparent from the resultant wake structure produced by the two wings. In root flapping wings, the term 'swirl' applies to the lateral motions of the wake. Although lateral motions are useful to some degree for the control of yaw moments, the energy that resides in the swirl is mainly wasteful because it does not contribute to the weight-supporting vertical momentum. The PIV analysis in Fig. 7 suggests, that the prominent lateral motions at −25% phase shift are redirected into the vertical when the wings flap with +25% phase shift. At +25% phase shift the wake is largely vertical, producing a conventional, converting momentum jet below the hind wing stroke plane. Since within the limits of the flow measurements the fluid velocity in the wake is smaller at +25% phase shift

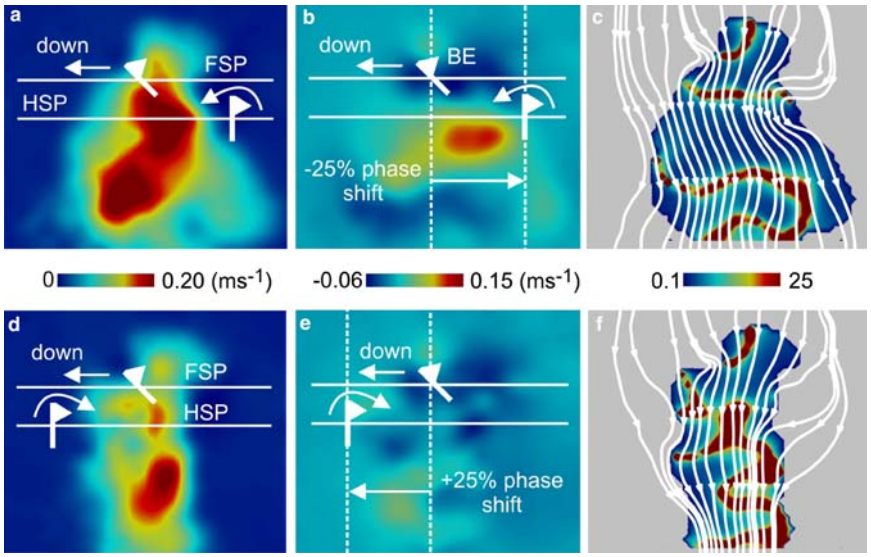

Fig. 7 Averaged wake patterns recorded at 25% forewing stroke cycle (single point measurement), at worst (−25%, fore wing leads wing motion, upper graphs) and best kinematic phase shift (+25% hind wing leads wing motion, lower graphs). See Fig. 2 for more information. **a**, **d** Vertical wake velocity for weight-supporting downwash, **b**, **e** absolute horizontal flow velocity and **c**, **f** ratio between vertical and horizontal velocity. Stream tubes, showing wake contraction in *f* compared to the wake expansion in **c**, indicate that less kinetic energy is wasted as swirl at positive, hind-wing leading phase shifts. Data are derived from two-dimensional digital particle image velocimetry in the region-of-interest shown in Fig. 2d. *Grey* indicates area in the wake at which vertical velocities are below 0.1 ms^{-1}. BE, blade element; FSP, fore wing-; HSP, hind wing stroke plane

compared to −25%, the kinetic energy put into the wake is less at the best phase shift, as already mentioned above. Thus, the power required to generate the mean lift for weight support is apparently reduced at best phase by a form of wing–wake interaction that broadly matches the prediction of Lan (1979) and also the findings by Wakeling and Ellington (1997b), who reported a +28% phase shift for dragonflies hovering freely at 0.21 advance ratio.

7 Conclusions

In this paper, we considered force production by insect tandem wings from the perspective of power expenditure and aerodynamic efficiency. Our finding that in four-winged insects, wing phasing determines both mean force production and power expenditures for flight, highlights the need of a comprehensive approach towards any explanations of how the various kinematic patterns of insect wings have evolved. Wing–wake interaction due to body motion is a common phenomenon during free-flight manoeuvring in insects and also occurs in two-winged hovering insects, for example, when the acceleration fields of the left and right wing interfere via the clap-and-fling mechanism. Detailed analyses of power expenditures and efficiency under the various flight conditions are widely missing and open a window for future research. Eventually, the finding that wing–wake interaction in root-flapping insect tandem wings is similar to the swirl removal mechanisms of contra-rotating propellers in helicopters and reconnaissance airplanes, such as the Kamov Ka-50 and the Avro Shackleton, respectively, is particularly valuable for engineers working on biomimetic aircraft design (Stafford 2007). Ellington (1999), for example, pointed out that flapping-winged aircrafts are challenged by the high power requirements for flapping flight. Any aerodynamic trick employed by insects to reduce energetic expenditures during flight should thus be of interest for both biologists and engineers.

Acknowledgments We would like to thank James Usherwood (The Royal Veterinary College, London) for his fruitful comments, Will Maybury for data collection and Ursula Seifert for critically reading the manuscript. This work was supported by grants Le905/6-1 and Le905/8-1 of the German Science Foundation (DFG).

References

Alexander DE (1984) Unusual phase relationships between the forewings and hindwings in flying dragonflies. J Exp Biol 109:379–383

Birch JM, Dickinson MH (2001) Spanwise flow and the attachment of the leading-edge vortex on insect wings. Nature 412:729–733

Birch JM, Dickinson MH (2003) The influence of wing–wake interactions on the production of aerodynamic forces in flapping flight. J Exp Biol 206:2257–2272

Casey TM (1989) Oxygen consumption during flight. In: Goldsworthy GJ, Wheeler CH (eds) Insect flight. CRC Press, Boca Raton, pp 257–272

Casey TM, Ellington CP (1989) Energetics of insect flight. In: Wieser W, Gnaiger E (eds) Energy transformations in cells and organisms. Thieme, Stuttgart, pp 200–210

Combes SA, Daniel TL (2003) Flexural stiffness in insect wings I. Scaling and the influence of wing venation. J Exp Biol 206:2979–2987

Dickinson MH, Lighton JRB (1995) Muscle efficiency and elastic storage in the flight motor of *Drosophila*. Science 268:87–89

Dickinson MH, Lehmann F-O, Sane S (1999) Wing rotation and the aerodynamic basis of insect flight. Science 284:1954–1960

Ellington CP (1984a) The aerodynamics of insect flight. VI. Lift and power requirements. Phil Trans R Soc Lond B 305:145–181

Ellington CP (1984b) The aerodynamics of insect flight. III. Kinematics. Proc R Soc Lond B 305:41–78

Ellington CP (1985) Power and efficiency of insect flight muscle. J Exp Biol 115:293–304

Ellington CP (1999) The novel aerodynamics of insect flight: applications to micro-air vehicles. J Exp Biol 202:3439–3448

Feuerbacher E, Fewell JH, Roberts SP, Smith EF, Harrison JF (2003) Effects of load type (pollen or nectar) and load mass on hovering metabolic rate and mechanical power output in the honey bee *Apis mellifera*. J Exp Biol 206:1855–1865

Ganguli R, Gorb S, Lehmann F-O (2008) Experiments on fly wing structure for biomimetic robotic flying insect design. AIAA 2008–1835

Gorb SN (1999) Serial elastic elements in the damselfly wing: mobile vein joints contain resilin. Naturwissenschaften 86:552–555

Gordon JE (1978) Structures: or why things don't fall down. Penguin Books, New York

Grodnitsky DL (1999) Form and function of insect wings: the evolution of biological structures. Johns Hopkins University Press, Baltimore

Josephson RK (1997) Power output from a flight muscle of the bumblebee Bombus terrestris: III. Power during simulated flight. J Exp Biol 200:1241–1246

King B (1993) Flight activity in the parasitoid wasp *Nasonia vitripennis* (Hymenoptera: Pteromalidae). J Insect Behav 6:313–321

Lan CE (1979) The unsteady quasi-vortex-lattice method with applications to animal propulsion. J Fluid Mech 93:747–765

Lan S, Sun M (2001) Aerodynamic force and flow structures of two airfoils in flapping motions. Acta Mech Sin 17:310–331

Langellotto GA, Denno RF, Ott JR (2000) A trade-off between flight capability and reproduction in males of a wing-dimorphic insect. Ecology 81:865–875

Lehmann F-O (2001) The efficiency of aerodynamic force production in *Drosophila*. J Comp Biochem Physiol A 131:77–88

Lehmann F-O (2008) When wings touch wakes: understanding locomotor force control by wake–wing interference in insect wings. J Exp Biol 211:224–233

Lehmann F-O, Dickinson MH (1997) The changes in power requirements and muscle efficiency during elevated force production in the fruit fly, *Drosophila melanogaster*. J Exp Biol 200:1133–1143

Lehmann F-O, Heymann N (2006) Dynamics of in vivo power output and efficiency of *Nasonia* asynchronous flight muscle. J Biotech 124:93–107

Lehmann F-O, Sane SP, Dickinson MH (2005) The aerodynamic effects of wing–wing interaction in flapping insect wings. J Exp Biol 208:2075–3092

Luttges MW (1989) Accomplished insect fliers. In: Gad-el-Hak M (ed) Frontiers in experimental fluid mechanics, Lecture Noted in Engineering. Springer, Berlin, pp 429–456

Maybury WJ, Lehmann F-O (2004) The fluid dynamics of flight control by kinematic phase lag variation between two robotic insect wings. J Exp Biol 207:4707–4726

Miller LA, Peskin CS (2004) When vortices stick: an aerodynamic transition in tiny insect flight. J Exp Biol 207:3073–3088

Moore JR (2006) Stretch activation: towards a molecular mechanism. In: Vigoreaux JO (ed) Nature's versatile engine: insect flight muscle inside and out. Landes Bioscience, Georgetown, pp 44–56

Norberg RA (1975) Hovering flight of the dragonfly *Aeschna juncea* L. In: Wu TY-T, Brokaw CJ, Brennen C (eds) Kinematics and aerodynamics, vol 2. Plenum Press, New York, pp 763–781

Prouty RW (2005) Helicopter performance, stability, and control. Kreiger, Malaba

Ramamurti R, Sandberg WC (2007) A computational investigation of the three-dimensional unsteady aerodynamics of *Drosophila* hovering and maneuvering. J Exp Biol 210:881–896

Reavis MA, Luttges MW (1988) Aerodynamic forces produced by a dragonfly. AIAA J 88-0330:1–13

Rüppell G (1989) Kinematic analysis of symmetrical flight manoeuvres of odonata. J Exp Biol 144:13–42

Saharon D, Luttges MW (1987) Three-dimensional flow produced by a pitching–plunging model dragonfly wing. AIAA J 87-0121:1–17

Saharon D, Luttges MW (1988) Visualization of unsteady separated flow produces by mechanically driven dragonfly wing kinematics model. AIAA J 88-0569:1–23

Saharon D, Luttges MW (1989) Dragonfly unsteady aerodynamics: the role of the wing phase relationship in controlling the produced flows. AIAA J 89-0832:1–19

Sane S, Dickinson MH (2001a) The control of flight force by a flapping wing: lift and drag production. J Exp Biol 204:2607–2626

Sane S, Dickinson MH (2001b) Erratum. J Exp Biol 204:3401

Sedov LI (1965) Two-dimensional problems in hydrodynamics and aerodynamics. Interscience Publishers, New York, pp 20–30

Srygley RB, Thomas ALR (2002) Unconventional lift-generating mechanisms in free-flying butterflies. Nature 420:660–664

Stafford N (2007) Spy in the sky. Nature 445:808–809

Sun M, Lan SL (2004) A computational study of the aerodynamic forces and power requirements of dragonfly (*Aeshna juncea*) hovering. J Exp Biol 207:1887–1901

Sun M, Tang J (2002) Unsteady aerodynamic force generation by a model fruit fly wing flapping motion. J Exp Biol 205:55–70

Thomas ALR, Taylor GK, Srygley RB, Nudds RL, Bomphrey RJ (2004) Dragonfly flight: free-flight and tethered flow visualizations reveal a diverse array of unsteady lift-generating mechanisms, controlled primarily via angle of attack. J Exp Biol 207:4299–4323

Usherwood JR, Ellington CP (2002) The aerodynamic of revolving wings I. Model hawkmoth wings. J Exp Biol 205:1547–1564

Usherwood JR, Lehmann F-O (2008) Phasing of dragonfly wings can improve aerodynamic efficiency by removing swirl. J R Soc Interface 1–6. doi:10.1098/rsif.2008.0124

Vandenberghe N, Zhang J, Childress S (2004) Symmetry breaking leads to forward flapping flight. J Fluid Mech 506:147–155

Wakeling JM, Ellington CP (1997a) Dragonfly Flight II. Velocities, accelerations, and kinematics of flapping flight. J Exp Biol 200:557–582

Wakeling JM, Ellington CP (1997b) Dragonfly flight III. Lift and power requirements. J Exp Biol 200:583–600

Wang ZJ, Russell D (2007) Effect of forewing and hindwing interactions on aerodynamic forces and power in hovering dragonfly flight. Phys Rev Lett 99. doi:10.1103/PhysRevLett.99.148101

Wang H, Zeng L, Liu H, Chunyong Y (2003) Measuring wing kinematics, flight trajectory and body attitude during forward flight and turning maneuvers in dragonflies. J Exp Biol 206:745–757

Weis-Fogh T (1972) Energetics of hovering flight in hummingbirds and in *Drosophila*. J Exp Biol 56:79–104

Weis-Fogh T (1973) Quick estimates of flight fitness in hovering animals, including novel mechanisms for lift production. J Exp Biol 59:169–230